

Scattering theory from artificial piezoelectric-like meta-atoms and molecules

Leonid Goltcman and Yakir Hadad*

School of Electrical Engineering, Tel-Aviv University, Ramat-Aviv, Tel-Aviv, Israel, 69978

(Dated: May 27, 2022)

Inspired by the natural piezoelectric effect, we introduce hybrid-wave electromechanical meta-atoms and meta-molecules that consist of coupled electrical and mechanical oscillators with similar resonance frequencies. We propose an analytical model for the linearized electromechanical scattering process, and explore its properties based on first principles. We demonstrate that by exploiting the linearized hybrid-wave interaction, one may enable functionalities that are forbidden otherwise, going beyond the limits of today's metamaterials. As an example we show an electrically deep sub-wavelength dimer of meta-atoms with extremely sensitive response to the direction-of-arrival of an impinging electromagnetic wave. This scheme of meta-atoms and molecules may open ways for metamaterials with a plethora of exciting dynamics and phenomena that have not been studied before with potential technological implications in radio-frequencies and acoustics.

PACS numbers: 43.35.+d, 77.84.-s, 41.20.Jb

Introduction.—The field of metamaterials, has gained a lot of attention in recent years for its potential in achieving effective material properties and functionalities that do not exist in nature [1, 2]. In the attempt to improve and enrich the performance of such effective materials, different types of meta-atoms, as well as lattice arrangements have been explored. These include electric or magnetic or combined [3, 4], anisotropic [5, 6], all-dielectric [7, 8], dynamic and time modulated [9, 10], nonlinear [11, 12], nonreciprocal [13–16], active and non-foster [17, 18], as well as mechanical and acoustical [16, 19–22] metamaterials. Hybrid-physics metamaterials that combine electromagnetic and mechanical properties are developed alongside other approaches for creating real time reconfigurable, tuneable, as well as nonlinear devices [23]. Utilizing thermal [24, 25], electrostatic [26–28], magnetic [29], and optical actuation [30–32] one can deform, on-demand and in fast rates, the metamaterial structure in the microscale and hence have superior control over its effective properties. Another type of man-made crystalline structures that involve hybrid-physics are the so called PhoXonic crystals [33]. Due to the very different velocities of light and sound, in a lattice of optomechanical cavities, an infrared photon and a gigahertz phonon have similar wavelength, hence giving rise to simultaneous photonic and phononic Bragg resonance and strong photon-phonon interaction. These and similar optomechanical structures have been extensively explored as nonlinear metamaterials [35], tuneable GHz resonators [36], for quantum processing [37, 38], as a mean for studying many body dynamics [39, 40], and quantum many body dynamics [41], as well as for long range synchronization [42].

As opposed to previous work, here we introduce hybrid-physics electromechanical meta-atoms and meta-molecules that consist of coupled electrical and mechanical oscillators with *similar* resonance frequencies, and that operate in a *linearizable* regime. We study the elec-

tromechanical scattering from these structures through a simple electromechanical response matrix, and explore its characteristics using first principles. We study small clusters and take advantage of the fact that an electrically small scatterer can be acoustically large to get functionalities that are forbidden otherwise. As an examples we show an ultra-sensitive electrically-deep-subwavelength direction-of-arrival sensor for electromagnetic waves.

The electromechanical meta-atom.—Wave scattering typically occurs at the same ‘physics’. For instance we have electromagnetic scattering, acoustic scattering, elastic scattering, and so on. Here, however, we consider an hybrid-physics scattering. An electromechanical (EMCL) scatterer partially transforms an impinging electromagnetic \mathbf{E}^i or acoustic \mathcal{P}^i waves into a mixture of acoustic and electromagnetic scattered waves \mathbf{E}^s and \mathcal{P}^s , as illustrated in Fig. 1a. This type of scattering exists in natural piezoelectric or photoelastic materials, however, it may be better controllable and efficient using artificial materials that involve EMCL coupled resonators. Such artificial materials are composed of lattices of EMCL meta-atoms. The latter, are excited by and radiate EMCL fields. We define an EMCL field as a four element vector containing the three electric field components and the scalar pressure field $\mathbf{U}(\mathbf{r}) = [E_x, E_y, E_z, \mathcal{P}]^T$. When an EMCL field impinges an EMCL meta-atom, electric and acoustic sources are induced, as illustrated in Fig. 1b. Assuming that the meta-atom is small enough compare to the wavelength of light and sound, the induced sources are appropriately modelled by coupled electric dipole \mathbf{p}_e and an acoustic monopole with volume \mathcal{V} (so that its *volume velocity* is $\mathcal{U} = \dot{\mathcal{V}}$). These constitute the EMCL source $\mathbf{S} = [p_{ex}, p_{ey}, p_{ez}, \mathcal{V}]^T$. Generally, the coupled EMCL problem is inherently nonlinear, however, in this work we restrict ourself to the class of problems that can be linearized under the weak signals assumption. The induced source \mathbf{S} is related to the impinging field \mathbf{U} at

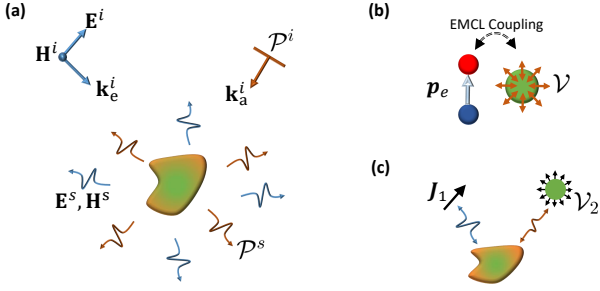


FIG. 1. (a) Illustration of the generalized hybrid-physics scattering process. An electromechanical meta-atom can be excited by both electromagnetic or acoustic fields, and it generally scatters the two type of waves regardless on the excitation. (b) If the resonators are electrically and acoustically small they compose a coupled system of electric dipole and acoustic monopole. Both radiate to the external ambient. (c) A configuration in which mutual action between the electric current source \mathbf{J}_1 and the acoustic pressure source \mathcal{V}_2 takes place via an EMCL meta-atom.

the meta-atom location via the linear response matrix,

$$\mathbf{S} = \underline{\underline{\alpha}}\mathbf{U}, \quad \text{with } \underline{\underline{\alpha}} = \begin{bmatrix} \underline{\underline{\alpha}}_{ee} & \underline{\underline{\alpha}}_{ea} \\ \underline{\underline{\alpha}}_{ae} & \underline{\underline{\alpha}}_{aa} \end{bmatrix}. \quad (1)$$

The diagonal terms are the common response terms in the absence of EMCL coupling. Specifically,

$$\underline{\underline{\alpha}}_{ee} = \begin{bmatrix} \alpha_{ee}^{xx} & \alpha_{ee}^{xy} & \alpha_{ee}^{xz} \\ \alpha_{ee}^{yx} & \alpha_{ee}^{yy} & \alpha_{ee}^{yz} \\ \alpha_{ee}^{zx} & \alpha_{ee}^{zy} & \alpha_{ee}^{zz} \end{bmatrix}, \quad \underline{\underline{\alpha}}_{aa} = \alpha_{aa} \quad (2)$$

where $\underline{\underline{\alpha}}_{ee}$ is the electric polarizability that describes the induced dipolar moment due to an impinging electromagnetic field, and $\underline{\underline{\alpha}}_{aa}$ gives the acoustic monopole volume induced by an impinging pressure field. The off-diagonal, EMCL coupling, terms in Eq. (1) read,

$$\underline{\underline{\alpha}}_{ea} = [\alpha_{ea}^x, \alpha_{ea}^y, \alpha_{ea}^z]^T, \quad \underline{\underline{\alpha}}_{ae} = [\alpha_{ae}^x, \alpha_{ae}^y, \alpha_{ae}^z]. \quad (3)$$

These terms are responsible for the direct and reverse piezoelectric-like behaviour of the meta-atom. Clearly, if the meta-atom exhibits no practical EMCL coupling then $\underline{\underline{\alpha}}_{ae} = \underline{\underline{\alpha}}_{ea} = 0$, and if in addition it is only electric (acoustic) then $\underline{\underline{\alpha}}_{aa} = 0$ ($\underline{\underline{\alpha}}_{ee} = 0$).

Going to the opposite direction, the field $\mathbf{U}(\mathbf{r})$ radiated by an induced source \mathbf{S} on a meta-atom at \mathbf{r}' is given by the EMCL Green's function $\mathbf{U}(\mathbf{r}) = \underline{\underline{G}}(\mathbf{r}, \mathbf{r}')\mathbf{S}$. Assuming that there is no EMCL interaction in the ambient medium, $\underline{\underline{G}}$ is block diagonal and reads

$$\underline{\underline{G}}(\mathbf{r}, \mathbf{r}') = \begin{bmatrix} \underline{\underline{G}}_e(\mathbf{r}, \mathbf{r}') & 0 \\ 0 & G_a(\mathbf{r}, \mathbf{r}') \end{bmatrix} \quad (4)$$

where $\underline{\underline{G}}_e$ (G_a) is the electric dyadic (acoustic scalar) Green's function connecting \mathbf{p}_e (\mathcal{V}) to \mathbf{E} (\mathcal{P}).

Fundamental constraints on $\underline{\underline{\alpha}}$.—The linear response matrix is subject to fundamental constraints due to reciprocity and energy conservation. We begin with reciprocity. Consider the hypothetical setup in Fig. 1c that contains an electric current \mathbf{J}_1 , acoustic monopole with volume velocity $\mathcal{U}_2 = \dot{\mathcal{V}}_2$, and an EMCL meta-atom. In the absence of the meta-atom, the interaction between the two sources is obviously zero. However, in the presence of the EMCL meta-atom, the electric field radiated by the current source \mathbf{J}_1 impinges the meta-atom, and consequently gives rise to scattering of both electromagnetic and acoustic pressure waves. The latter, denoted here by \mathcal{P}_1 , interacts with the acoustic source \mathcal{U}_2 , implying that this time an action $\mathcal{A}[\mathbf{J}_1 \rightarrow \mathcal{U}_2] = \mathcal{P}_1\mathcal{U}_2$ between the sources takes place. In the reciprocal scenario the acoustic source \mathcal{U}_2 acts on \mathbf{J}_1 through the scattered electromagnetic field \mathbf{E}_2 , $\mathcal{A}[\mathcal{U}_2 \rightarrow \mathbf{J}_1] = \mathbf{E}_2 \cdot \mathbf{J}_1$. Since we deal with a linearized system the mutual action between the sources should be equal [43],

$$\mathcal{A}[\mathbf{J}_1 \rightarrow \mathcal{U}_2] = \mathcal{A}[\mathcal{U}_2 \rightarrow \mathbf{J}_1]. \quad (5)$$

Expressing Eq. (5) using the electromagnetic and acoustic Green's functions, we find

$$\begin{aligned} \mathcal{U}_2 G_a(\mathbf{r}_2, \mathbf{r}_s) \underline{\underline{\alpha}}_{ea} \underline{\underline{G}}_e(\mathbf{r}_s, \mathbf{r}_1) \mathbf{J}_1 = \\ \mathbf{J}_1^T \underline{\underline{G}}_e(\mathbf{r}_1, \mathbf{r}_s) \underline{\underline{\alpha}}_{ae} G_a(\mathbf{r}_s, \mathbf{r}_2) \mathcal{U}_2. \end{aligned} \quad (6)$$

Assuming that the medium is electromagnetically and acoustically reciprocal, $\underline{\underline{G}}_e(\mathbf{r}, \mathbf{r}') = \underline{\underline{G}}_e^T(\mathbf{r}', \mathbf{r})$ [44], $G_a(\mathbf{r}, \mathbf{r}') = G_a(\mathbf{r}', \mathbf{r})$ [43]. Then with Eq. (6) we find

$$\underline{\underline{\alpha}}_{ea} = \underline{\underline{\alpha}}_{ae}^T. \quad (7)$$

This symmetry is a manifestation of the principle of microscopic reversibility [45, 46] applied to the linearized meta-atom system.

Next, we consider energy conservation. In the absence of material losses of any kind, the power that an impinging EMCL field \mathbf{U} extracts for the excitation of the induced source \mathbf{S} on the meta-atom is equal to the total EMCL radiated power by the meta-atom. The extracted EMCL power reads $P^{ext} = (\omega/2)\text{Im}\{\mathbf{U}^H \underline{\underline{\alpha}}^H \mathbf{U}\}$ where superscript H denotes the Hermitian transpose [47]. On the other hand, the total radiated power reads $P^{rad} = \mathbf{U}^H \underline{\underline{\alpha}}^H \underline{\underline{\chi}} \underline{\underline{\alpha}} \mathbf{U}$ with $\underline{\underline{\chi}} = \text{diag}[I_{3 \times 3}, P_e^{rad}, P_a^{rad}]$. Where $I_{3 \times 3}$ is the 3 by 3 unitary matrix, and P_e^{rad} , P_a^{rad} are the total power radiated by an electromagnetic dipole, and an acoustic monopole, both of unit amplitudes [47]. For a meta-atom embedded in a homogeneous medium with permittivity and permeability ϵ and μ , and with density ρ_0 we have $P_e^{rad} = \mu\omega^4/12\pi c_e$ [48] and $P_a^{rad} = \rho_0\omega^4/8\pi c_a$ [49], where c_e and c_a are, respectively, the speed of light and sound in the medium. If the medium is more complex, the radiation terms should be corrected accordingly. For instance, for a meta-atom embedded in an ,electromagnetic transparent, acoustic

hard-wall duct with cross section area A_d that supports only plane wave we have $P_a^{rad} = \rho\omega^2 c_a/4A_d$ [49], while P_e^{rad} unchanged. By equating $P^{ext} = P^{rad}$ we find that $\underline{\alpha}$ is subject to

$$\underline{\underline{\alpha}}^H \underline{\underline{\chi}} \underline{\alpha} = (\omega/4j)[\underline{\underline{\alpha}}^H - \underline{\underline{\alpha}}]. \quad (8)$$

This is a generalization of the optical theorem [1, 44].

Schematic realization of EMCL meta-atom.—Consider a parallel plate capacitor with nominal capacitance C_0 loaded by an inductor L to establish an electromagnetic resonance at frequency $\omega_e = 1/\sqrt{LC_0}$. Simultaneously, each capacitor plate acts as a membrane that mechanically resonates at $\omega_m = \sqrt{k/m}$ where m , and k , are the membrane's effective mass and stiffness. We assume that the capacitor volume between the plates is acoustically closed, and thus it responds mechanically to external pressure changes. See Fig. 2a for illustration. The system is set at equilibrium by applying a biasing voltage V_0 , yielding to static charge accumulation, q_0 and $-q_0$, and thereby to a constant Coulomb attraction force between the plates. In the absence (presence) of the static biasing the spacing between the plates is d ($d - x_0$). Neglecting edge effects, we define the nominal capacitance as $C_0 = \epsilon_c A/(d - x_0)$ where ϵ_c is the permittivity between the plates, and A is the plate area.

The meta-atom can be excited by either electromagnetic or acoustic wave as illustrated in Fig. 2a. Using the concept of effective length in antenna theory [48], the impinging electromagnetic wave excitation is modelled by a lumped voltage source, $v(t) = l_{\text{eff}} E_x^i(t)$. Here, E_x^i is the electric field component normal to the plates and l_{eff} is the effective length of the capacitor when viewed as an electrically small antenna. Once excited, the meta-atom can be described effectively by an electric dipole $\mathbf{p}_e = p_e \hat{x}$ with $p_e = l_{\text{eff}} \delta q$, coupled to an acoustic monopole with volume $\mathcal{V} = A\delta x$ (volume velocity $\mathcal{U} = \dot{\mathcal{V}} = A\dot{\delta x}$) [43].

The temporal dynamics is inherently nonlinear [47]. However, if the excitation is weak enough compared to static biasing so that $\delta q \ll q_0$, then the meta-atom response can be linearized around its equilibrium,

$$\ddot{\delta q} + 2\tau_e^{-1} \dot{\delta q} + \omega_e^2 \delta q = L^{-1}[v(t) + E_0 \delta x], \quad (9a)$$

$$\ddot{\delta x} + 2\tau_m^{-1} \dot{\delta x} + \omega_m^2 \delta x = m^{-1}[f(t) + E_0 \delta q]. \quad (9b)$$

Here τ_e^{-1} and τ_m^{-1} are the electromagnetic and mechanical decay rates that include radiation as well as material damping, ω_e and ω_m are defined earlier, and $E_0 = -V_0/(d - x_0)$ is the static electric field between the capacitor plates. The coupling terms in Eqs. (9) have a clear physical meaning. In Eq. (9a) the small signal deflection δx yields effectively an extra voltage source $E_0 \delta x$, and in Eq. (9b) the small signal charge δq creates an extra force between the plates $E_0 \delta q$.

The charge fluctuations δq create an effective electric dipolar moment $p_e = l_{\text{eff}} \delta q$, normal to the capacitor plates (along \hat{x}). Moreover, the displacement fluctuations

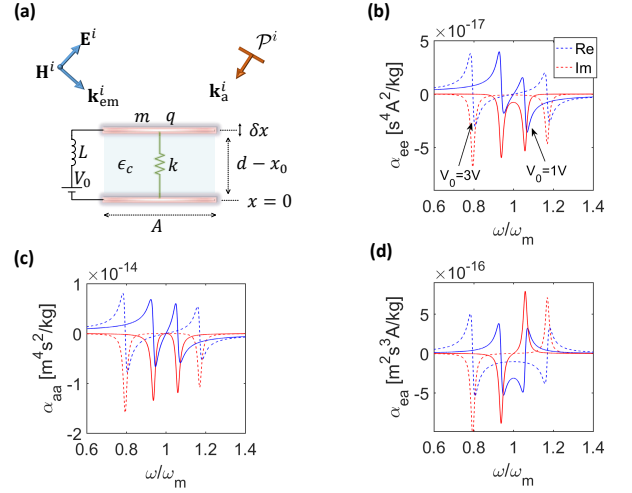


FIG. 2. (a) A parallel plate EMCL meta-atom, set at its operation point by a bias voltage V_0 , and can be excited by electromagnetic or acoustic fields. Its EMCL small signal (linear) dispersion with frequency is given in (b-d). Blue (red) line denotes real (imaginary) part. Continuous (dashed) line corresponds to biasing voltage $V_0 = 1V$ ($V_0 = 3V$). (b) The electric polarizability - α_{ee} , (c) the acoustic response - α_{aa} - the induced acoustic monopole due to a local acoustic pressure field, (d) the EMCL coupling terms - $\alpha_{ae} = \alpha_{ea}$ - induced electric dipole (acoustic monopole) due to a local acoustic pressure (electric) field.

δx give rise to an effective acoustic monopole source with volume oscillations amplitude $\mathcal{V} = A\delta x$ and volume velocity $\mathcal{U} = j\omega\mathcal{V}$ (here and henceforth, time dependence $e^{j\omega t}$ is assumed and suppressed). Finally, the system's linear response is expressed in the form of Eq. (1), with

$$\alpha_{ee} = (l_{\text{eff}}^2/\Delta L) [\omega_m^2 - \omega^2 + 2j\omega/\tau_m] \quad (10a)$$

$$\alpha_{aa} = (A_{\text{eff}}^2/\Delta m) [\omega_e^2 - \omega^2 + 2j\omega/\tau_e] \quad (10b)$$

$$\alpha_{ea} = \alpha_{ae} = l_{\text{eff}} A_{\text{eff}} E_0 / \Delta L m \quad (10c)$$

and where

$$\Delta = \left(\omega_e^2 - \omega^2 + \frac{2j\omega}{\tau_e} \right) \left(\omega_m^2 - \omega^2 + \frac{2j\omega}{\tau_m} \right) - \frac{E_0^2}{Lm}. \quad (11)$$

In this example, the meta-atom responds only to an x -polarized electric field, and therefore $\underline{\underline{\alpha}}_{ee}, \underline{\underline{\alpha}}_{ea}, \underline{\underline{\alpha}}_{ae}$ are all scalars. Note the symmetry $\alpha_{ea} = \alpha_{ae}$ as dictated in Eq. (7) by reciprocity. Moreover, assuming that the meta-atom is lossless (namely, only radiation loss is allowed), using Eq. (8) we find

$$\begin{aligned} \omega \Im\{\alpha_{ee}^{-1}\}/2 &= P_e^{rad} + |\alpha_{ae}/\alpha_{ee}|^2 P_a^{rad} \\ \omega \Im\{\alpha_{aa}^{-1}\}/2 &= P_a^{rad} + |\alpha_{ea}/\alpha_{aa}|^2 P_e^{rad} \end{aligned} \quad (12)$$

and $\Im\{\alpha_{ee}^* \alpha_{ea}\} = \Im\{\alpha_{aa}^* \alpha_{ae}\} = \Im\{\alpha_{ee}^* \alpha_{aa}\} = 0$. The latter three constraints are related to the mathematical structure of the linear response matrix, whereas the first two constraints given in Eq. (12) can be solved to find

the decay rates τ_e^{-1} and τ_m^{-1} . In the absence of static biasing, $V_0 = 0$, and therefore $\alpha_{ae} = \alpha_{ea} = 0$, implying no EMCL coupling. In this case, the relations in Eq. (12) are reduced to the conventional constraint of the polarizability of a small scatterer due to the optical theorem, and to its acoustic analog. By plugging Eqs. (10,11) into Eq. (12), we get a nonlinear system that is solved for τ_e , and τ_m , yielding

$$\tau_e = \omega^2 L / l_e^2 P_e^{rad}, \quad \tau_m = \omega^2 m / A_e^2 P_a^{rad}. \quad (13)$$

The decay rates are proportional to the radiated power and hence the balance between τ_e and τ_m can be considerably tuned by appropriate engineering of the meta-atom ambient medium. Since at a given frequency ω , $\lambda_e = 2\pi c_e / \omega \gg \lambda_a = 2\pi c_a / \omega$, a meta-atom that its typical size is in the order of $\sim \lambda_a$ will be electrically deep subwavelength $\ll \lambda_e$. Therefore, typically, the electromagnetic radiation efficiency will be considerably smaller than its acoustic counterpart, implying that the electromagnetic resonance dominates since $\tau_e \gg \tau_m$. To make these rates comparable one may excite higher order acoustic multipoles that are less efficient radiators, or reduce the ambient medium density. However the greatest control over the meta-atom decay rates will be obtained by placing it in an acoustic or electromagnetic duct or cavity with a suitably engineered local density of states. The latter idea is demonstrated in Fig.2(b-d) where the elements of the response matrix are plotted as function of frequency for the meta-atom in Fig. 2(a) with $\omega_e = \omega_m = 2\pi \times 10^6$ rad/s, $A_{\text{eff}} = 3.14 \mu\text{m}^2$, $l_{\text{eff}} = 10 \mu\text{m}$, $m = 4.2 \mu\text{g}$, $L = 1 \mu\text{H}$, that is embedded in an, electromagnetically transparent, hard-wall acoustic duct with cross section $A_d = 5A_{\text{eff}}$ that supports an acoustic plane wave only. The mechanical parameters are taken close to [50]. Here, $\tau_e \sim \tau_m$ and the system is in the strong coupling regime. The coupling tunability via the static biasing voltage is demonstrated with $V_0 = 1\text{V}$ and $V_0 = 3\text{V}$.

Highly-sensitive electrically small direction-of-arrival sensor.—The EMCL meta-atoms discussed above can be used to design a piezoelectric-like meta-molecules with superior performance due to the joint acoustical and electromagnetic properties. As an interesting example we design a system of two meta-atoms inside a duct that is centered along the \hat{y} axis, and with parameters as used for Fig.2(b-d). We excite the system only by an electromagnetic wave impinging at incidence angle θ_i , so that $\mathbf{U}^i = [E_x^i, 0]^T$ with $E_x^i = E_0 \exp[-jk_e(\cos\theta_i \hat{y} - \sin\theta_i \hat{z})]$ ($k_e = \omega/c_e$). The electric field polarization \hat{x} normal to the meta-atoms plates. See Fig. 3(a). We set the separation between the meta-atoms d to be electrically deep sub-wavelength $d \ll \lambda_e$ while acoustically large $d \gg \lambda_a$. The dynamics of the coupled system is given by

$$\begin{aligned} \mathbf{S}_1 &= \underline{\underline{G}}(\mathbf{r}_1, \mathbf{r}_2) \mathbf{S}_2 + \mathbf{U}^i(\mathbf{r}_1) \\ \mathbf{S}_2 &= \underline{\underline{G}}(\mathbf{r}_2, \mathbf{r}_1) \mathbf{S}_1 + \mathbf{U}^i(\mathbf{r}_2) \end{aligned} \quad (14)$$

where $\mathbf{S}_1, \mathbf{S}_2$ are the EMCL excitation amplitudes of the meta-atoms located at $\mathbf{r}_1 = -d/2\hat{y}$ and $\mathbf{r}_2 = d/2\hat{y}$. The Green's functions used here are given in [47]. It is instructive to consider the corresponding eigenvalue problem alongside with the excitation one. To find the eigenfrequencies we set $\mathbf{U}^i = 0$, and require non-trivial solutions in Eq.(14). In the absence of the EMCL coupling, the system reduces to a simple coupled dipoles that support two resonances, bright and dark, with eigenfrequencies nearly independent of $d \ll \lambda_e$. In this case, an impinging electromagnetic plane wave cannot practically excite the dark mode but only its bright counterpart. Fig. 3(b) shows the ratio $|p_1/p_2|$ (in log scale) as function of the incidence angle θ_i and the normalized frequency $\Delta\omega/\omega_c$ (where $\Delta\omega = \omega - \omega_c$), about the dark resonance ω_c . Even near the dark resonance $\omega_c = 0.985458\omega_m$, there is neither a practical difference between the excitation amplitude of the dipoles, nor effect when varying the incidence angle θ_i . Here, as opposed to a conventional direction-of-arrival sensor with two antennas separated by $d \sim \lambda_e/2$ [48], the phase difference between the received signals in the two antennas $\sim k_e d$ is extremely small since $d \ll \lambda_e$. However, we boost the small phase effect by utilizing the presence of EMCL coupling. Since the structure is acoustically large the number of eigenfrequencies is significantly larger, and their complex values strongly depend on d . A typical complex- ω plane showing the resonance locations is given in the inset inside Fig. 3(c) for $d/\lambda_m = 30$ where $\lambda_m = 2\pi c_a / \omega_m$. In Fig. 3(c) the loci of several complex eigenfrequencies are plotted with d as a parameter that its value is color encoded ($\Im\{\omega\}$ is in log scale to emphasize the resonance distinct locations). There are two families of eigenfrequencies that correspond to number of bright and dark modes (see upper inset). As an example, we set $d = 28\lambda_m \approx 9.24\text{mm}$ and find low loss dark resonance at $\omega_c = 0.92846\omega_m$. When exciting the structure with an electromagnetic plane wave at frequencies about the dark resonance, the dark resonance interplays with the bright resonance and give rise to very strong variation of the excitation amplitudes as function of the incidence angle θ_i as shown in Fig. 3(d,e). This correlation can be used to estimate the direction of arrival. Moreover, in this scheme, a measurement of the excited acoustic field, as opposed to the electromagnetic field that can be overwhelmed by the impinging wave, may increase detection sensitivity and noise fidelity.

Conclusions.—Here we discussed a paradigm for tuneable piezoelectric-like metamaterials and utilized the fact that an electrically small scatterer is usually acoustically large, giving rise to hybrid-wave resonances that are unique to the electromechanical wave system. This concept with the other results in the paper may pave the way towards a plethora of new exciting dynamics and phenomena that have not been studied before and that may lead to technological implications in radio-frequencies and acoustics, such as ultra sensitive detectors, super-

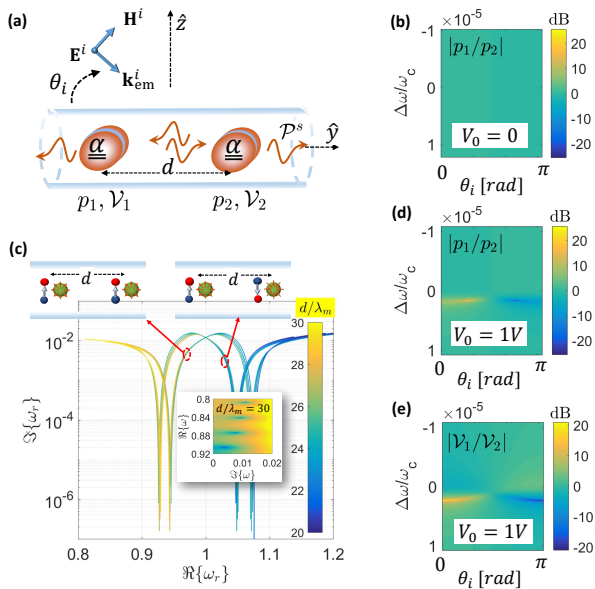


FIG. 3. (a) Illustration of an electrically deep subwavelength direction-of-arrival sensor for an electromagnetic wave. (b) In the absence of EMCL coupling, $V_0 = 0$, only the bright mode can practically be excited and therefore the excitation of the two electric dipoles is practically identical for all θ_i . (c) Evolution of the complex resonance frequencies as the spacing d between the meta-atoms varies. There are two families of resonances that correspond to bright and dark EMCL states (upper inset) (d) As the electromechanical coupling is turned on, $V_0 = 1V$, the electric dipole excitation highly depends on θ_i , (e) and similarly the acoustic excitation response.

resolution imaging, and highly non-reciprocal devices.

The Tel-Aviv University rector startup fund is acknowledged.

* hadady@eng.tau.ac.il

- [1] N. Engheta and R. W. Ziolkowski (editors). *Metamaterials: Physics and Engineering Explorations*. Wiley-IEEE Press, 2006.
- [2] F. Capolino (editor). *Theory and Phenomena of Metamaterials*. CRC Press, 2009.
- [3] A. Alu and N. Engheta, “The quest for magnetic plasmons at optical frequencies,” *Opt. Express*, **17** (7), 57235730 (2009).
- [4] W.-C. Chen, C. M. Bingham, K. M. Mak, N. W. Caira, and W. J. Padilla, “Extremely subwavelength planar magnetic metamaterials,” *Phys. Rev. B* **85**, 201104(R) (2012).
- [5] P. B. Catrysse and S. Fan. “Routing of deep-subwavelength optical beams and images without reflection and diffraction using infinitely anisotropic metamaterials,” *Adv. Mat.*, **25** (2), 194198 (2013).
- [6] D. Van Orden, Y. Fainman, and V. Lomakin, “Twisted chains of resonant particles: optical polarization control, waveguidance, and radiation,” *Opt. Lett.*, **35** (15), 25792581 (2010).
- [7] James C. Ginn *et al*, “Realizing Optical Magnetism from Dielectric Metamaterials” *Phys. Rev. Lett.* **108**, 097402 (2012)
- [8] D. Lin, P. Fan, E. Hasman, and Mark L. Brongersma, “Dielectric gradient metasurface optical elements,” *Science*, **345** (6194), 298302 (2014).
- [9] Y. Hadad, J. C. Soric, and A. Alu, “Breaking temporal symmetries for emission and absorption,” *Proc. Nat. Acad. Sci.*, **113** (13), 34713475 (2016).
- [10] K. Fan and Willie J. Padilla, “Dynamic electromagnetic metamaterials,” *Materials Today*, **18**, (1) (2015).
- [11] P.-Y. Chen and A. Alu, “Optical nanoantenna arrays loaded with nonlinear materials,” *Phys. Rev. B*, **82**, 235405 (2010).
- [12] D. F. Sievenpiper, “Nonlinear grounded metasurfaces for suppression of high-power pulsed rf currents,” *IEEE Antennas and Wireless Propagation Letters*, **10**, 15161519 (2011).
- [13] Y. Hadad and Ben Z. Steinberg, “Magnetized spiral chains of plasmonic ellipsoids for one-way optical waveguides,” *Phys. Rev. Lett.*, **105**, 233904 (2010).
- [14] T. Kodera, D. L. Sounas, and C. Caloz, “Magnetless Nonreciprocal Metamaterial (MNM) Technology: Application to Microwave Components,” *IEEE Trans. Microwave Theory and Techniques*, **61** (3) (2013)
- [15] Y. Mazor and Ben Z. Steinberg, “Metaweaves: Sectorway nonreciprocal metasurfaces,” *Phys. Rev. Lett.*, **112**, 153901 (2014).
- [16] C. Coulais, D. Sounas, and A. Alu, “Static non-reciprocity in mechanical metamaterials,” *Nature* **542**, 461464 (2017).
- [17] H. Mirzaei and G. V. Eleftheriades, “Realizing non-foster reactive elements using negative-group delay networks,” *IEEE Trans. Microwave Theory and Techniques*, **61**, (12), 4322-4332 (2013).
- [18] J. Long and D. F. Sievenpiper, “Low-profile and low-dispersion artificial impedance surface in the uhf band based on non-foster circuit loading,” *IEEE Trans. Ant. Prop.*, **64** (7), 30033010 (2016).
- [19] R. Fleury and A. Alu, “Extraordinary sound transmission through density-near-zero ultranarrow channels,” *Phys. Rev. Lett.*, **111**, 055501 (2013).
- [20] L. M. Nash *et al*, “Topological mechanics of gyroscopic metamaterials,” *Proc. Nat. Acad. Sci.*, **112** (47), 1449514500 (2015).
- [21] J. Paulose, A. S. Meeussen, and V. Vitelli, “Selective buckling via states of self-stress in topological metamaterials,” *Proc. Nat. Acad. Sci.*, **112** (25), 76397644 (2015).
- [22] A. B. Khanikaev, R. Fleury, S. H. Mousavi, and A. Alu, “Topologically robust sound propagation in an angular-momentum-biased graphene-like resonator lattice,” *Nat. Comm.*, **6**, 8260:1 7 (2015).
- [23] N. I. Zheludev, and E. Plum, “Reconfigurable nanomechanical photonic metamaterials,” *Nat. Nanotech* **11**, 16-22, DOI:10.1038 (2016)
- [24] H. Tau *et al*, “Reconfigurable terahertz metamaterials,” *Phys. Rev. Lett.* **103**, 147401 (2009)
- [25] J. Ou, E. Plum, L. Jiang, and N. I. Zheludev, “Reconfigurable photonic metamaterials,” *Nano Lett.*, **11**, 2142-2144 (2011).
- [26] D. Chicherin *et al*, “MEMS-based high impedance surfaces for millimeter and submillimeter wave applications,” *Microw. Opt. Technol. Lett.*, **48**, 2570-2573 (2006).

- [27] T. Hand and S. Cummer, "Characterization of tuneable metamaterial elements using MEMS switches," *IEEE Antenn. Wireless Prop. Lett.*, **6**, 401-404 (2007).
- [28] W. M. Zhu *et al.*, "Switchable magnetic metamaterials using micromachining processes," *Adv. Mater.* **23**, 1792-1796 (2011)
- [29] J. Valente, J. Ou, E. Plum, I. J. Youngs, and N. I. Zheludev, "Reconfiguring photonic metamaterials with currents and magnetic fields," *App. Phys. Lett.* **106**, 111905 (2015).
- [30] R. Zhao, P. Tassin, T. Koschny, C. M. Soukoulis, "Optical forces in nanowire pairs and metamaterials," *Opt. Express* **18**, 25665-25676 (2010).
- [31] M. Lapine, I. V. Shadrivov, D. A. Powell, and Y. S. Kivshar, "Magnetoelastic metamaterials," *Nat. Mater.* **11**, 3033 (2012).
- [32] A. Karvounis, J. Y. Ou, W. Wu, K. F. MacDonald, N. I. Zheludev, "Nano-optomechanical nonlinear dielectric metamaterials," *Appl. Phys. Lett.* **107**, 191110 (2015)
- [33] M. Eichenfield, J. Chan, R. M. Camacho, K. J. Vahala, and O. Painter, "Optomechanical crystals," *Nature* **462** (7269), 7882 (2009).
- [34] A. H. Safavi-Naeini and O. Painter, "Design of optomechanical cavities and waveguides on a simultaneous bandgap phononic-photonic crystal slab," *Opt. Express* **18** (14), 1492614943 (2010).
- [35] M. Schmidt, V. Peano, and F. Marquardt, "Optomechanical metamaterials: Dirac polaritons, Gauge fields, and instabilities," *arXiv:1311.7095* (2013).
- [36] H. Pfeifer, T. Paraso, L. Zang, and O. Painter, "Design of tunable GHz-frequency optomechanical crystal resonators," *Opt. Exp.* **24** (11), 11407-11419 (2016).
- [37] M. Schmidt, M. Ludwig, and F. Marquardt, "Optomechanical circuits for nanomechanical continuous variable quantum state processing," *New J. Phys.* **14** (12), 125005 (2012).
- [38] V. Peano, C. Brendel, M. Schmidt, and F. Marquardt, "Topological phases of sound and light," *Phys. Rev. X* **5** (3), 031011 (2015).
- [39] E. Buks and M. L. Roukes, "Electrically tunable collective response in a coupled micromechanical array," *Journal of Microelectromechanical Systems*, **11** (6), 802807 (2002).
- [40] R. Lifshitz and M. C. Cross, "Response of parametrically driven nonlinear coupled oscillators with application to micromechanical and nanomechanical resonator arrays," *Phys. Rev. B*, **67**, 134302 (2003).
- [41] M. Ludwig and F. Marquardt, "Quantum many-body dynamics in optomechanical arrays," *Phys. Rev. Lett.* **111** (7), 073603 (2013).
- [42] S. Y. Shah, M. Zhang, R. Rand, and M. Lipson, "Master-slave locking of optomechanical oscillators over a long distance," *Phys. Rev. Lett.*, **114**, 113602 (2015).
- [43] L. E. Kinsler and A. R. Frey, *Fundamentals of Acoustics*, 2nd Ed., John Wiley & Sons (1962).
- [44] J. D. Jackson, *Classical Electrodynamics*. Wiley: New York, 1998.
- [45] G. N. Lewis, "A new principle of equilibrium," *PNAS*, **11**, 179-183 (1921).
- [46] L. Onsager, "Reciprocal relations in irreversible processes, I," *Phys. Rev.*, **15** (37) (1931).
- [47] Supplementary Material available online.
- [48] C. A. Balanis, *Modern Antenna Handbook*, John Wiley & Sons (2008).
- [49] A. D. Pierce, *Acoustics - An introduction to its physical principles and applications*, 3rd Ed., Acoustical Society of America (1991) [p. 161, p. 319].
- [50] P.-L. Yu, Y.P. Purdy and C.A. Regal, "Control of material damping in high-q membrane microresonators," *Phys. Rev. Lett.*, **108**:083603 (2012).

Supplementary Material for “Scattering theory from artificial piezoelectric-like meta-atoms and molecules”

Leonid Goltcman and Yakir Hadad*

School of Electrical Engineering, Tel-Aviv University, Ramat-Aviv, Tel-Aviv, Israel, 69978

(Dated: May 27, 2022)

While the main text is written to be basically self-contained, there are some minor gaps that are less critical for the clear understanding of the message but are important for the reproduction of the paper results. These few items are described below for the sake of completeness.

CONTENTS

I. Derivation of the extracted electromechanical power	1
II. Derivation of the total radiated power from an EMCL meta-atom	1
III. Lumped sources model for the parallel plates meta-atom	2
IV. Derivation of the parallel plates meta-atom dynamics	2
V. Electromagnetic and acoustic Green’s function used	3

I. DERIVATION OF THE EXTRACTED ELECTROMECHANICAL POWER

The power that an electromechanical wave $\mathbf{U} = [\mathbf{E}, \mathcal{P}]^T$ extracts to excite an electromechanical meta-atom with induced source $\mathbf{S} = [\mathbf{p}_e, \mathcal{V}]^T$ is given by

$$P^{ext} = \frac{1}{2} \Re\{\mathbf{J}^* \cdot \mathbf{E} + \mathcal{U}^* \mathcal{P}\} \quad (\text{S1})$$

where $\mathbf{J} = j\omega\mathbf{p}_e$ is the current source associated with the induced electric dipole on the scatterer, and $\mathcal{U} = j\omega\mathcal{V}$ is the volume velocity associated with the monopole volume amplitude \mathcal{V} . Then, we have,

$$P^{ext} = \frac{\omega}{2} \Im\{\mathbf{p}_e^* \cdot \mathbf{E} + \mathcal{V}^* \mathcal{P}\} = \frac{\omega}{2} \mathbf{S}^H \mathbf{U}. \quad (\text{S2})$$

However, since $\mathbf{S} = \underline{\alpha} \mathbf{U}$ (Eq. (1) in the main text), we can write

$$P^{ext} = \frac{\omega}{2} \Im\{(\underline{\alpha} \mathbf{U})^H \mathbf{U}\} = \frac{\omega}{2} \Im\{\mathbf{U}^H \underline{\alpha}^H \mathbf{U}\}. \quad (\text{S3})$$

This completes the derivation of the extracted power given in the main text.

II. DERIVATION OF THE TOTAL RADIATED POWER FROM AN EMCL META-ATOM

The total radiated power from an EMCL source \mathbf{S} in electromagnetically as well as acoustically homogeneous medium reads

$$P^{rad} = \frac{\rho\omega^4}{8\pi c_a} \mathcal{V}^* \mathcal{V} + \frac{\mu\omega^4}{12\pi c_e} \mathbf{p}_e^* \cdot \mathbf{p}_e. \quad (\text{S4})$$

* hadady@eng.tau.ac.il

For a general medium, however, although the coefficients in the equation above will be changed, the square dependence on $\mathcal{V}^*\mathcal{V}$ and $\mathbf{p}_e^* \cdot \mathbf{p}_e$ will be maintained. Therefore, we define (as in the main text) P_a^{rad} and P_e^{rad} as the total radiated power for acoustic monopole and electromagnetic dipole sources with unit amplitude, namely, with $|\mathcal{V}| = 1$ and $|\mathbf{p}_e| = 1$. Then, by defining

$$\underline{\underline{\chi}} = \text{diag}[P_e^{rad}, P_e^{rad}, P_e^{rad}, P_a^{rad}] = \text{diag}[P_e^{rad} \underline{\underline{I}}_{3 \times 3}, P_a^{rad}]. \quad (\text{S5})$$

we obtain the expression given in the main text for the radiated power,

$$P^{rad} = \mathbf{U}^H \underline{\underline{\alpha}}^H \underline{\underline{\chi}} \underline{\underline{\alpha}} \mathbf{U}. \quad (\text{S6})$$

III. LUMPED SOURCES MODEL FOR THE PARALLEL PLATES META-ATOM

For the parallel plate meta-atom discussed in Fig. 2(a) of the main text the impinging electric and pressure fields are modelled using lumped sources. The sources excitation scheme is shown in Fig. S1 below.

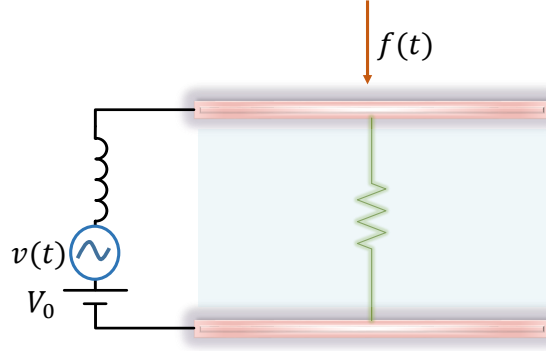


FIG. S1. Lumped excitation model

IV. DERIVATION OF THE PARALLEL PLATES META-ATOM DYNAMICS

The meta-atom dynamics is captured by the Lagrangian

$$\mathcal{L} = \frac{1}{2}m\dot{x}^2 - \frac{1}{2}kx^2 + \frac{1}{2}L\dot{q}^2 - \frac{1}{2} \frac{q^2}{C(x)}, \quad (\text{S7})$$

with source \mathcal{L}_s and dissipation \mathcal{F} functionals

$$\mathcal{L}_s = qV + xf, \quad \mathcal{F} = \frac{1}{2}R\dot{q}^2 + \frac{1}{2}B\dot{x}^2 \quad (\text{S8})$$

where $V = V_0 + v(t)$, $x = -x_0 + \delta x$ (x_0 is taken such that $x_0 > 0$), and $q = q_0 + \delta q$ are the plate's deflection and charge accumulation, respectively. The dissipation term \mathcal{F} includes two loss mechanisms, electromagnetic and mechanical, represented, respectively, by resistance R and viscosity B , where both consist of radiation as well as material loss channels. Using Eqs.(S7)-(S8) in the Lagrange equations we obtain the relations between the static quantities, x_0, q_0, V_0 , as well as relations between the small signal terms $\delta x, \delta q, v(t), f(t)$, that represent the temporal dynamics. For the static terms we find $q_0 = C_0 V_0$, $kx_0 = q_0^2 / 2\epsilon A$ which are nothing but the voltage-charge relation on the capacitor, and equality of forces between the spring repulsion due to contraction of x_0 and the Coulomb attraction between the plates of capacitor charged with q_0 . Assuming that $x_0 \ll d$ we may approximate $x_0 \approx \epsilon AV_0 / 2kd^2$ and $q_0 \approx \epsilon AV_0 / d$.

For the dynamic terms we find the following nonlinear system

$$\ddot{\delta q} + 2\tau_e^{-1}\dot{\delta q} + \omega_e^2 \left(q_0 \frac{\delta x}{d - x_0} + \delta q + \frac{\delta x}{d - x_0} \delta q \right) = \frac{1}{L} v(t), \quad (\text{S9})$$

and

$$\ddot{\delta x} + 2\tau_m^{-1}\dot{\delta x} + \omega_m^2 \delta x + \frac{1}{m} \frac{V_0}{d - x_0} \delta q + \frac{1}{2} \frac{\delta q^2}{C_0} \frac{1}{m(d - x_0)} = \frac{1}{m} f(t). \quad (\text{S10})$$

Here $\tau_e^{-1} = R/2L$ and $\tau_m^{-1} = B/2m$ are the electromagnetic and mechanical damping rates, ω_e and ω_m are the electromagnetic and mechanical resonance frequencies in the absence of electromechanical coupling between the resonators, and $E_0 = -V_0/(d - x_0)$ is the average electric field between the capacitor plates due to the static biasing. Eq. (9) in the main text is derived from the nonlinear system above under the assumption that $\delta q \ll q_0$ and $\delta x \ll x_0$.

V. ELECTROMAGNETIC AND ACOUSTIC GREEN'S FUNCTION USED

The electromagnetic Green's function in electromagnetically homogeneous medium with permittivity and permeability ϵ and μ is used in the calculation of the dimer response in Eq. (14) of the main text. It reads

$$\underline{\underline{G}}_e(\mathbf{r}, \mathbf{r}') = \frac{e^{-jk_e r}}{4\pi\epsilon} \left\{ \underline{\underline{A}} \frac{k_e^2}{r} + [3\underline{\underline{B}} - \underline{\underline{I}}_{3 \times 3}] \left(\frac{1}{r^3} + \frac{jk_e}{r^2} \right) \right\} \quad (\text{S11})$$

with

$$\underline{\underline{A}} = \begin{bmatrix} n_y^2 + n_z^2 & -n_x n_y & -n_x n_z \\ -n_x n_y & n_x^2 + n_z^2 & -n_z n_y \\ -n_z n_x & -n_z n_y & n_x^2 + n_y^2 \end{bmatrix} \quad (\text{S12})$$

and

$$\underline{\underline{B}} = \begin{bmatrix} n_x^2 & n_x n_y & n_x n_z \\ n_x n_y & n_y^2 & n_z n_y \\ n_z n_x & n_z n_y & n_z^2 \end{bmatrix} \quad (\text{S13})$$

where $\underline{\underline{I}}_{3 \times 3}$ is the 3 by 3 unitary matrix, $r = |\mathbf{r} - \mathbf{r}'|$ is the distance between the source and observer points, and $\hat{n} = (n_x, n_y, n_z) = (\mathbf{r} - \mathbf{r}')/r$ is the unit vector pointing between the source and the observer. Moreover, $k_e = \omega/c_e$ where c_e is the speed of light. For the dimer problem considered in the last part of the paper we had $\hat{n} = (0, \pm 1, 0)$ and $\mathbf{p}_{1,2} = p_{1,2} \hat{x}$.

The acoustic Green's function we used in that example was the Green's function of small acoustic monopole source in a duct supporting a plane wave only at the operation frequency (fundamental mode of the duct). In this case, since the driving frequency is below the cutoff of the higher order modes, the latter decays away from the source. Therefore, sufficiently far from the source (in terms of acoustic wavelength $d \gg \lambda_a$), we can asymptotically approximate the acoustic Green's function by

$$G_a \sim \frac{-j\omega\rho c_a}{2A_d} e^{-jk_a r} \quad (\text{S14})$$

where here r is the distance between the source and the observer along the duct axis. In the main text this is the \hat{y} axis and the distance between the two meta-atoms ranged between $d = 20\lambda_m$ and $d = 30\lambda_m$, in any case satisfying the asymptotic assumption requirement. Moreover $k_a = \omega/c_a$, where c_a is the speed of sound in the duct and A_d is the duct cross section area.